Supporting Information

Understanding Synergistic Enhanced Thermocatalytic Decomposition of Ammonium Perchlorate by Cobalt Nanoparticles-embedded Nitrogen-doped Graphitized Carbon

Hong Lin,[a] Qingchun Zhang,[a,b,*] Huiyu Liu,[a] Shiying Shen,[b,*] Zhiliang Guo,[a] Bo Jin,[a,*] Rufang Peng[a]

[a] *State Key Laboratory of Environment-friendly Energy Materials, School of Materials Science and Engineering, Southwest University of Science and Technology, Mianyang 621010, P. R. China*

[b] *Institute of Applied Physics and Materials Engineering, University of Macau, Macao SAR, 999078, P. R. China*

* *Corresponding authors: zhangqingchun@swust.edu.cn (Q. Zhang), shiyingshen@um.edu.mo (S. Shen), jinbo0428@163.com (B. Jin); Tel.: +86-816-2419011*

1 Experimental Section

1.1 Materials and Equipment. All the reagents and solvents used were all of the analytical grades and without further purification. 2-methylimidazole and $Co(NO_3)_2 \cdot 6H_2O$ were purchased from Aladdin Biochemical Technology Co., Ltd. (Shanghai, China). Methanol was purchased from Chengdu Colon Chemical Co., Ltd. (Chengdu, China).

The X-ray diffraction (XRD) patterns were tested by a PANalytical X'Pert Pro X-ray diffractometer with monochromatized Cu K_α. The microscopic morphologies were observed by Zeiss Supra 55VP field emission scanning electron microscope (FE-SEM) and Zeiss Libra 200 transmission electron microscope (TEM). The differential thermal analysis (DTA) was determined by using a WCR-2B differential thermal analyzer. The X-ray photoelectron spectroscopy (XPS) was used Al K_α radiation to collect on scanning X-ray microprobe (Thermo ESCALAB 250XI, USA). The Brunner-Emmett-Teller (BET) surface areas and porous structure was measured using the ASAP 2460 volumetric analyzer from the N_2 adsorption-desorption isotherm at 77 K. The inductively coupled plasma optical emission spectrometry (ICP-OES) was carried out with Agilent 5110. The precise weighing was carried on a Sartorius BT25S analytical balance that was accurate to 0.01 mg.

1.2 The Preparation of ZIF-67 and Co-NPs@NC-*T*. The ZIF-67 was prepared according to a previously reported method with little modifying[1]. First, $Co(NO_3)_2 \cdot 6H_2O$（5.82 g, 20.0 mmol）and 2-methylimidazole (6.16 g, 75.0 mmol) were separately dissolved in methanol (150 mL), and then which were mixed and continued to stir for 24 h under room temperature. The precipitates were collected by centrifuge and dried in a drying oven at 60 ^oC for 12 h to obtained ZIF-67 as purple power.

The Co-NPs@NC-*T* was prepared by calcining ZIF-67. The ZIF-67 precursor was placed in a tube

furnace and heated to 600 ℃, 800 ℃, and 1000 ℃ with a heating rate of 5 ℃ min^{-1}, and then keep it constant for 2 h under argon atmosphere to respectively obtain Co-NPs@NC-600, Co-NPs@NC-800, and Co-NPs@NC-1000 as black power.

1.3 Thermal Analysis. The DTA was carried out with a WCR-2B differential thermal analyzer. The samples of AP with 2 wt%, 4 wt%, 6 wt%, 8 wt%, and 10 wt% Co-NPs@NC-*T* or ZIF-67 were prepared by careful addition of Co-NPs@NC-*T* or ZIF-67 in pure AP, and then the samples (3 mg) were respectively used for DTA test under a temperature range from room temperature to 500 °C with a heating rate of 10 K min^{-1} and a nitrogen atmosphere flow with a rate of 35 mL min^{-1}. The samples (3 mg) of pure AP and AP with 10 wt% Co-NPs@NC-*T* or ZIF-67 were used for DTA test under a temperature range from room temperature to 500 °C with a heating rate of 2, 5, 10, 15, and 20 K min^{-1} and a nitrogen atmosphere flow with a rate of 35 mL min^{-1}. The peak temperature of DTA was used to determine the kinetic parameters by Kissinger's method[2]. The integral area of the exothermic peak of DTA was used to determine the heat release.

1.4 DFT Calculations. All spin-polarized first-principles DFT calculations were performed using the Vienna ab initio simulation package. In order to describe the ion-electron interactions, projector-augmented wave (PAW) potentials were adopted. The Perdew-Burke-Ernzerhof (PBE) exchange-correlation functional within the generalized gradient approximation (GGA) was employed[3-6]. The energy cut-off for the plane-wave basis was set to 450 eV. A 3×3×1 grid k-point mesh by the Monkhorst-Pack method is used for geometry optimization and the static total energy calculations.[5] The influence of 3d electrons of Co atoms was considered and a DFT + U method was used as an on-site Coulomb correction. The parameter of (U-J) was set to 3.3 eV, which has been confirmed as a suitable value to avoid large computational resources without absurd results[7, 8]. To take into account the van der Waals interactions, the dispersion corrected DFT-D3 method was used[9]. The convergence thresholds for energy and atomic forces were set as 10^{-4} eV and 0.02 eV $Å^{-1}$, respectively.

2 Figures and Tables

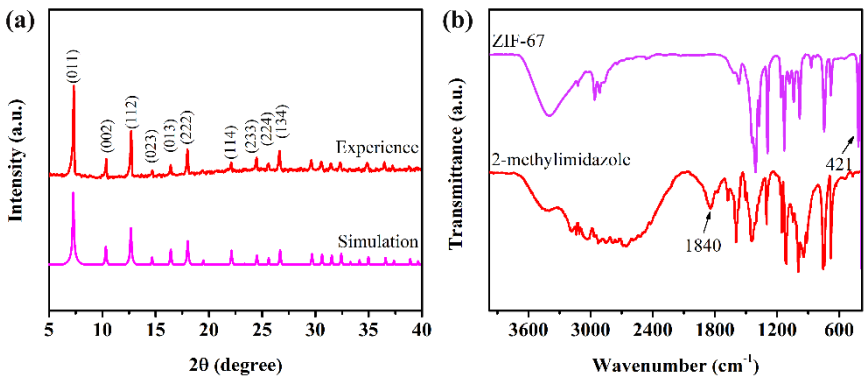

Figure S1. a) The experimental and simulative XRD of ZIF-67 precursor. b) The FTIR of ZIF-67 precursor and 2-

methylimidazole.

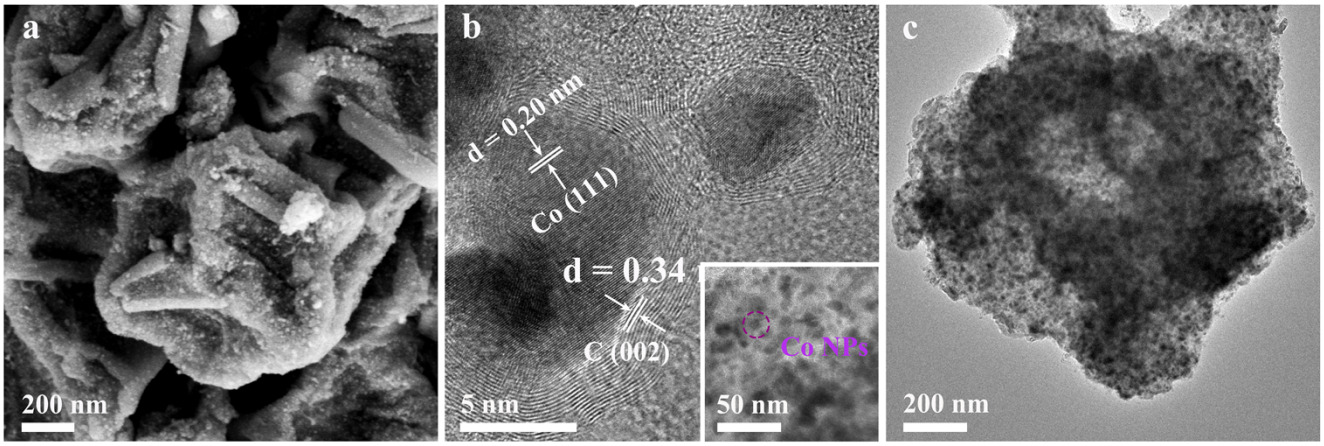

Figure S2. a) SEM, b) HRTEM, and c) TEM of Co-NPs@NC-600.

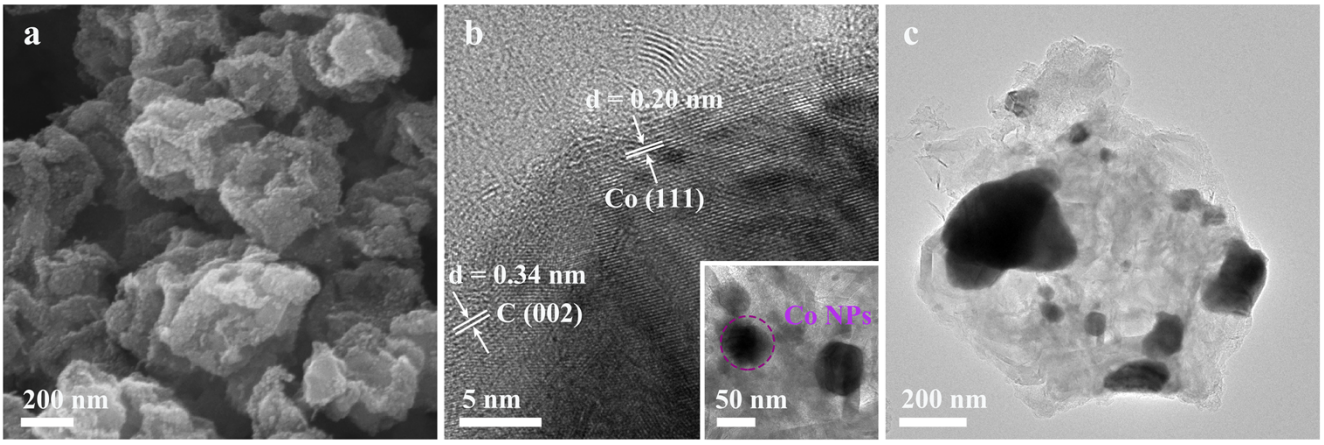

Figure S3. a) SEM, b) HRTEM, and c) TEM of Co-NPs@NC-1000.

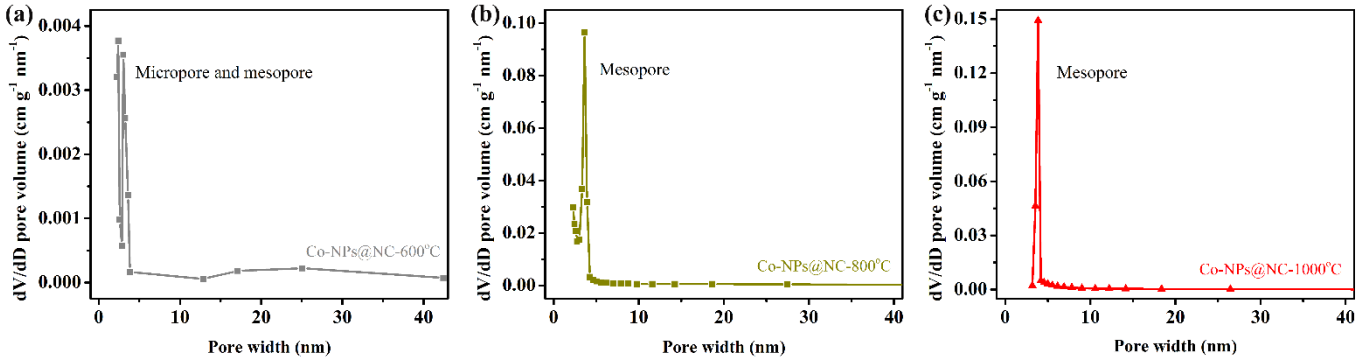

Figure S4. The pore size distributions of a) Co-NPs@NC-600, b) Co-NPs@NC-800, and c) Co-NPs@NC-1000.

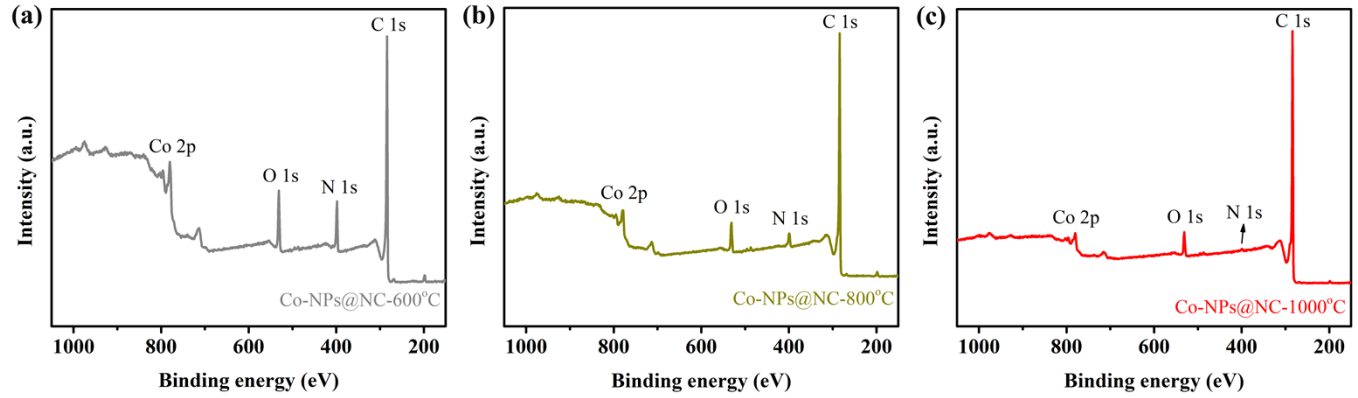

Figure S5. The XPS survey of a) Co-NPs@NC-600, b) Co-NPs@NC-800, and c) Co-NPs@NC-1000.

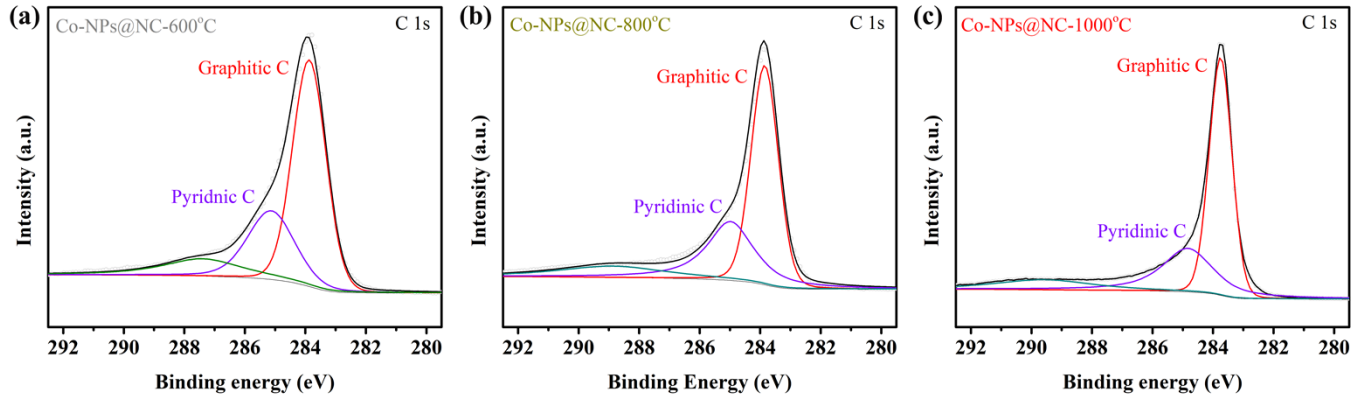

Figure S6. The high-resolution C 1s spectra of a) Co-NPs@NC-600, b) Co-NPs@NC-800, and c) Co-NPs@NC-1000.

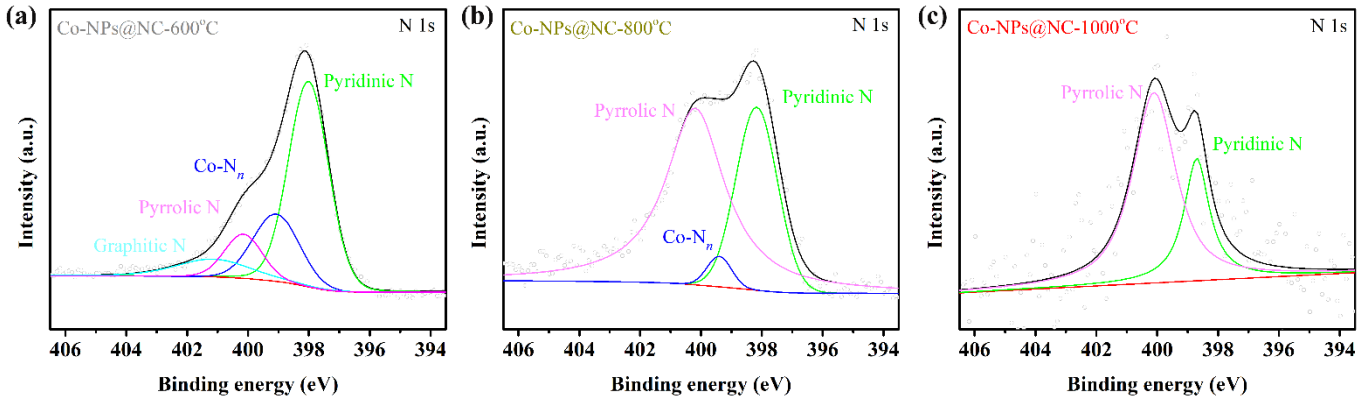

Figure S7. The high-resolution N 1s spectra of a) Co-NPs@NC-600, b) Co-NPs@NC-800, and c) Co-NPs@NC-1000.

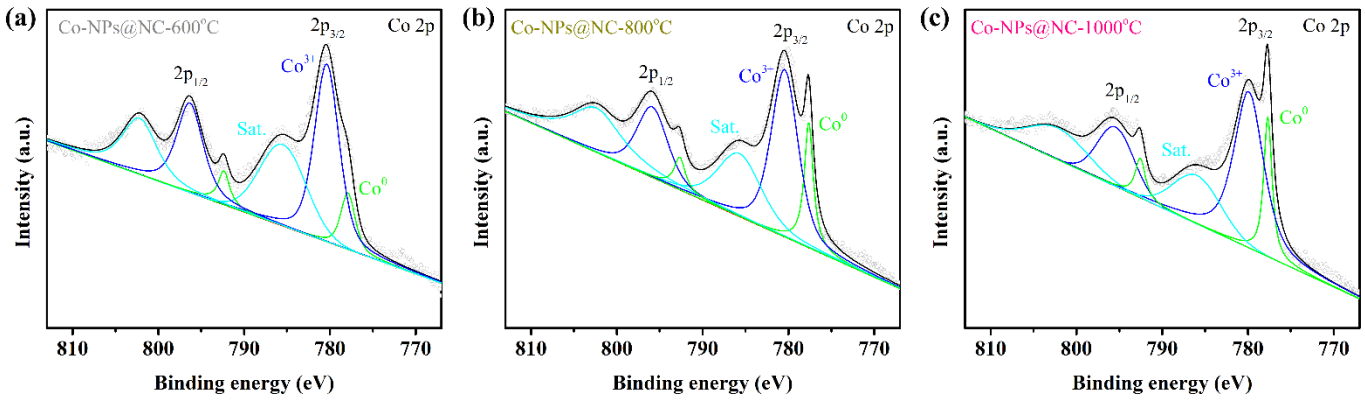

Figure S8. The high-resolution Co 2p spectra of a) Co-NPs@NC-600, b) Co-NPs@NC-800, and c) Co-NPs@NC-1000.

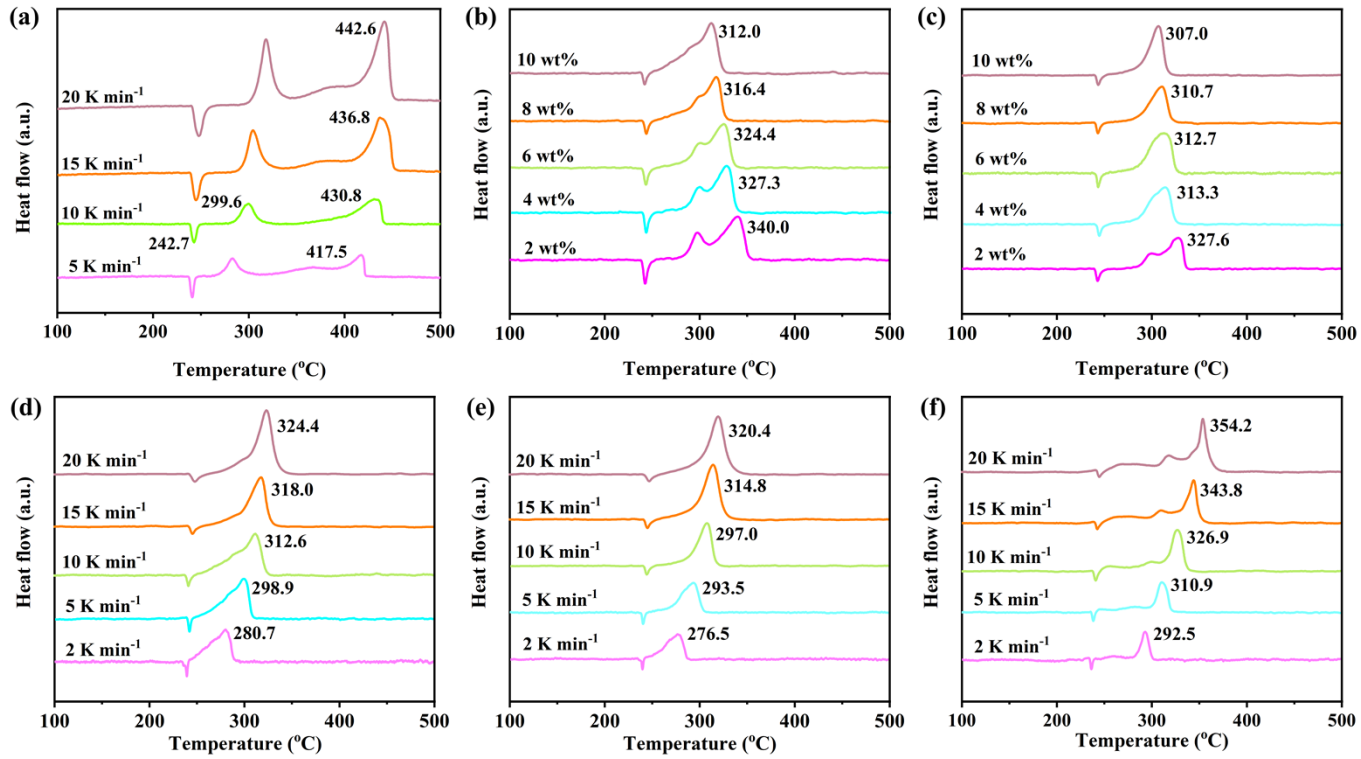

Figure S9. a) The DTA curves of pure AP at different heating rates. The DTA curves of AP with different contents of b) Co-NPs@NC-600, c) Co-NPs@NC-1000 at a heating rate of 10 K min^{-1}. The DTA curves of AP with 10 wt% d) Co-NPs@NC-600, e) Co-NPs@NC-1000, and (f) ZIF-67 at different heating rates.

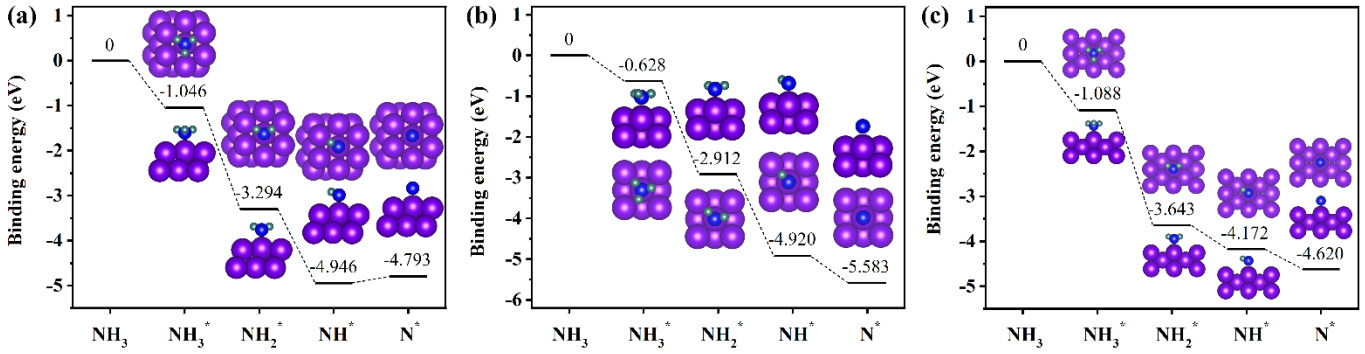

Figure S10. The binding energy and optimized structures of NH_3 and its dissociated species on a) (111) plane, b) (200) plane, and c) (220) plane of Co-NPs. The violet, blue, and green balls respectively represent Co, N, and H atoms.

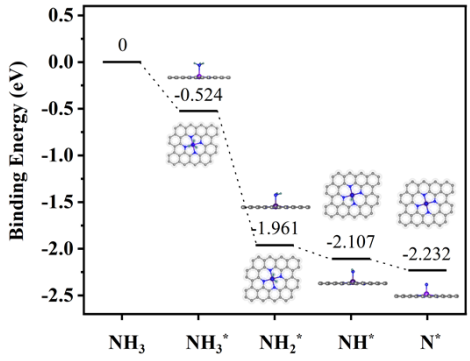

Figure S11. The binding energy and optimized structures of NH_3 and its dissociated species on CoN_4 site of Co-SAs@NC. The violet, gray, blue, and green balls respectively represent Co, C, N, and H atoms.

Table S1. The element contents of Co-NPs@NC-*T* were measured by XPS and ICP-OES.

Catalysts	XPS			ICP-OES
	Carbon (at%)	Nitrogen (at%)	Cobalt (at%)/(wt%)	Cobalt (wt%)
Co-NPs@NC-600	82.5	12.3	5.2/26.4	37.8
Co-NPs@NC-800	92.0	5.3	2.7/13.5	43.3
Co-NPs@NC-1000	96.7	1.3	2.0/10.0	56.9

Table S2. The HTD peak integral area of pure AP, ZIF-67, and Co-NPs@NC-*T*/AP

Catalysts	Content (wt%)	Heating rate (K min^{-1})	Integral area
Pure AP	/	10	109.1
ZIF-67	10	10	372.4
Co-NPs@NC-600	10	10	513.3
Co-NPs@NC-800	10	10	594.0
Co-NPs@NC-1000	10	10	437.6

References

1. Li, X.; Li, Z.; Lu, L.; Huang, L.; Xiang, L.; Shen, J.; Liu, S.; Xiao, D. R. The Solvent Induced Inter-Dimensional Phase Transformations of Cobalt Zeolitic-Imidazolate Frameworks. *Chemistry-A European Journal* **2017,** 23 (44), 10638-10643 DOI: 10.1002/chem.201701721.
2. Kissinger, H. E. Reaction kinetics in differential thermal analysis. *Analytical Chemistry* **1957,** 29 (11), 1702-1706. DOI: 10.1021/ac60131a045
3. Kresse, G.; Furthmüller, J. Efficient iterative schemes for ab initio total-energy calculations using a plane-wave basis set. *Physical Review B* **1996,** 54 (16), 11169-11186 DOI: 10.1103/PhysRevB.54.11169.
4. Kresse, G.; Joubert, D. From ultrasoft pseudopotentials to the projector augmented-wave method. *Physical Review B* **1999,** 59 (3), 1758-1775 DOI: 10.1103/PhysRevB.59.1758.
5. Blöchl, P. E. Projector augmented-wave method. *Physical Review B* **1994,** 50 (24), 17953-17979 DOI: 10.1103/PhysRevB.50.17953.
6. Moellmann, J.; Grimme, S. DFT-D3 Study of Some Molecular Crystals. *The Journal of Physical Chemistry C* **2014,** 118 (14), 7615-7621 DOI: 10.1021/jp501237c.
7. Dudarev, S. L.; Botton, G. A.; Savrasov, S. Y.; Humphreys, C. J.; Sutton, A. P. Electron-energy-loss spectra and the structural stability of nickel oxide: An LSDA+U study. *Physical Review B* **1998,** 57 (3), 1505-1509 DOI: 10.1103/PhysRevB.57.1505.
8. Shojaee, K.; Haynes, B. S.; Montoya, A. The catalytic oxidation of NH_3 on Co_3O_4(110): A theoretical study. *Proceedings of the Combustion Institute* **2017,** 36 (3), 4365-4373 DOI: 10.1016/j.proci.2016.06.100.
9. Liechtenstein, A. I.; Anisimov, V. I.; Zaanen, J. Density-functional theory and strong interactions: Orbital ordering in Mott-Hubbard insulators. *Physical Review B* **1995,** 52 (8), R5467-R5470 DOI: 10.1103/PhysRevB.52.R5467.